Exploring Non-Hermitian Topological Quantum Phenomenon

Siddhant Midha
Department of Electrical Engineering
Indian Institute of Technology Bombay, Powai, Mumbai *
(Dated: November 27, 2022)

The past few years have witnessed rapid developments in the theoretical and experimental foundations of topological quantum phenomenon and the topology of bandstructures. Further, there has also been interest in understanding non-hermitian quantum systems owing to their generality and usefulness in understanding a variety of physical systems . This review paper aims to elucidate the notion of this topology in non-hermitian systems owing to recent theoretical work done in this arena – from the meaning of the fundamental geometric phase in a system with a non-hermitian hamiltonian, to the breakdown of the famous bulk-boundary correspondence (BBC) in these systems. Key ideas such as the Non-Hermitian Skin Effect (NHSE), Exceptional Points (EPs) are discussed, and examples along with necessary figures are given.

I. INTRODUCTION

When one thinks about the fundamentals of quantum mechanics, one naturally thinks about a Hilbert Space $\mathcal{H}$ on which is defined a hermitian operator called the Hamiltonian H. Quantum systems are described by statevectors $|\psi\rangle \in \mathcal{H}$ through the ever-familiar Schroedinger Equation,

$$\iota\hbar\frac{\partial |\psi\rangle}{\partial t} = H|\psi\rangle$$

The hermiticity of the hamiltonian plays two key roles, viz., unitarity of the time evolution and the reality of the energy eigenvalues. The first role is due to the fact that probability must be conserved, and the second corresponds to the fact that experimentally observed energies have to be real. But, in [1] the authors have shown that for acheiving these two conditions, hermiticity of the hamiltonian is *not* a necessary requirement. Further, they showed that it can be replaced by the more general and more physical requirement of $\mathcal{PT}$ Symmetry - that is, invariance under space and time inversion. This not only validated the earlier infamous works with non-hermitian (NH) hamiltonians, but also inspired research in the analysis of NH systems. Non hermiticity is useful for understanding many physical systems, for instance, optic systems with gain and loss [2], in open systems [3] [4] and in solid state systems [5].

In parallel, the quest for understanding the nature of topology in condensed matter systems has been quite driven. A key consequence of this phenomenon is the existence of robust boundary (surface/edge) zero states which are immune to perturbation [6, 7]. The nature of these boundary states has been found to be intimately linked with the topological properties of the bulk hamiltonian when working with the translational invariant bloch theory. This relation is referred to as the Bulk Boundary Correspondence (BBC), and is a fundamental idea in the theory of topological insulators.

As we have seen, many physical systems are more amenable to analysis with a non-hermitian hamiltonian. This creates a natural inclination to explore the aforementioned topological phenomenon in non-hermitian systems. In the subsequent sections, we see that the results seen after application of the usual hermitian theory to these systems turn out to be wildly unexpected. Notably, we see a complete breakdown of the BBC in non-hermitian systems. Further, we see a particular charecteristic of non-hermitian systems, which is the Non-Hermitian Skin Effect (NHSE). This entails a phenomenon where all (many) bulk states have exponentially decaying amplitudes into the bulk.

We organize this review as follows. First, we stress upon the formalisms involved in analyzing NH systems and review two salient features of NH systems – Exceptional Points, and Symmetry Ramifications. Then, we review the basic meaning of the foundational aspect of all the topological business – the geometric phase (the berry phase) in NH systems. Further, we conduct some numerical investigations to show the BBC and the NHSE, and follow up by a review of topological analysis of the NHSE and a generalized NH-BBC. Finally, we discuss some models and the ways in which topology in NH systems has been explained.

II. ANALYZING NH SYSTEMS

A. The Basic Formalism

Given a NH system, we have a hamiltonian such that $H \neq H^\dagger$. Assuming no degeneracies for simplicity, it has been shown that ([8], [9]) there exist sets of vectors $\{|\psi_R^n\rangle : n\}$ and $\{|\psi_L^n\rangle : n\}$ such that,

$$\begin{aligned} H|\psi_R^n\rangle &= E_n|\psi_R^n\rangle \\ H^\dagger|\psi_L^n\rangle &= E_n^*|\psi_L^n\rangle \end{aligned} \tag{1}$$

* siddhantm@iitb.ac.in

Such that,

$$\begin{aligned} \langle \psi_L^n \mid \psi_R^m \rangle &= \delta_{mn} \\ \sum_n |\psi_L^n\rangle \langle \psi_R^n| &= 1 \end{aligned} \tag{2}$$

This is what is called a *Biorthogonal Quantum System*. Note that the right eigenstates do not form an orthogonal system, but they are linearly independent. One can expand a general state in either of the basis, viz,

$$\begin{aligned} |\psi\rangle &= \sum_n c_n |\psi_R^n\rangle \\ |\psi\rangle &= \sum_n d_n |\psi_L^n\rangle \end{aligned} \tag{3}$$

Furthermore, the authors of [10] showed that, given such a biorthogonal quantum system, there is guaranteed the existence of a hermitian matrix X such that

$$|\psi_L^n\rangle = X |\psi_R^n\rangle \text{ for all } n \tag{4}$$

With this, they define the now invariant norm as,

$$\langle \psi, \psi \rangle_X \equiv \langle \psi \mid X \mid \psi \rangle \tag{5}$$

for any $|\psi\rangle \in \mathcal{H}$.

B. Exceptional Points

NH Systems with parametrized hamiltonians possess an interesting property of the existence of exceptional points. These are points in the parameter space where the hamiltonian matrix is defective – that is, it cannot be diagonalized. This is in contrast to a *genuine* degeneracy in the hermitian case. Formally, at exceptional points we have that the geometric multiplicity of atleast one eigenvalue is less than the algebraic multiplicity (See Appendix).

We illustrate EPs with an example. Consider the parametrized hamiltonian [11]

$$H(\alpha) = \begin{pmatrix} 0 & \alpha \\ 1 & 0 \end{pmatrix} \qquad \alpha \in \mathbb{C} \tag{6}$$

It has the complex spectrum,

$$E_\pm = \pm\sqrt{\alpha} \quad |\psi_R^\pm\rangle = \begin{pmatrix} \pm\sqrt{\alpha} \\ 1 \end{pmatrix} \quad |\psi_L^\pm\rangle = \begin{pmatrix} 1 \\ \pm\sqrt{\alpha} \end{pmatrix} \tag{7}$$

Here we have an EP at $\alpha = 0$. The eigenvectors and eigenvalues *coalesce* at the EP, reducing $H(\alpha = 0)$ to a Jordan Block form. The effect of this EP can be seen by traversing closed loops in the α space – if one traverses a loop which contains the EP ($\alpha = 0$), a *switching* of the eigenenergies and the eigenstates takes place. This hints towards a Mobius Loop Structure. Moreover, we have that the eigenspectrum is not analytic at the EPs.

We illustrate this with a $3-D$ example, based on the work in [12].

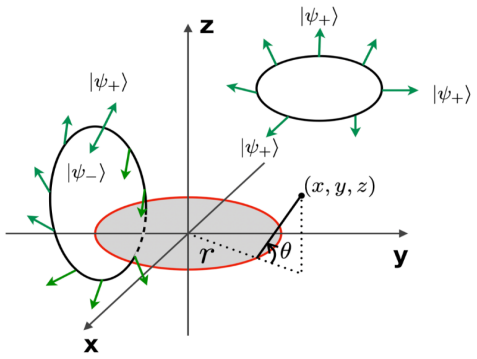

FIG. 1: Mobius Loops in Hermitian Systems [12]

1. *Mobius Loops in Hermitian Systems*

Consider the the *hermitian* two-level hamiltonian,

$$H_e(\theta) = \cos\left(\frac{\theta}{2}\right)\left[\cos\left(\frac{\theta}{2}\right)\sigma_z + \sin\left(\frac{\theta}{2}\right)\sigma_x\right], \tag{8}$$

where $0 \leqslant \theta \leqslant 2\pi$ is defined as,

$$\theta = \begin{cases} \arccos\left(\frac{\sqrt{x^2+y^2}-r}{\sqrt{\left(\sqrt{x^2+y^2}-r\right)^2+z^2}}\right) & \text{if} \quad z \geqslant 0 \\ 2\pi - \arccos\left(\frac{\sqrt{x^2+y^2}-r}{\sqrt{\left(\sqrt{x^2+y^2}-r\right)^2+z^2}}\right) & \text{if} \quad z < 0 \end{cases} . \tag{9}$$

The eigenenergies of H_e are $E_\pm(\theta) = \pm\cos\left(\frac{\theta}{2}\right)$ and the corresponding eigenstates are

$$|\psi_R^+(\theta)\rangle = \begin{pmatrix} \cos\frac{\theta}{4} \\ \sin\frac{\theta}{4} \end{pmatrix}, |\psi_R^-(\theta)\rangle = \begin{pmatrix} -\sin\frac{\theta}{4} \\ \cos\frac{\theta}{4} \end{pmatrix} \tag{10}$$

The system is degenerate on the whole shaded disk (See Figure 1). Consider two loops, one which is disjoint from any degeneracy and one which touches the degeneracy disk. When we move along these loops in an adiabatic fashion, we can keep track of the particular eigenket if we are *not* touching any degenerate points. On the other hand, encountering a degeneracy leads to a switching in the eigenket. This gives a mobius loop structure.

2. *Mobius Loops in NH Systems*

Consider a simple NH hamiltonian

$$H = p_x\sigma_x + p_y\sigma_y + (p_z + \mathrm{i}s)\,\sigma_z \tag{11}$$

parametrized by $\mathbf{p} = (p_x, p_y, p_z)$. The real parameter s controls the non-Hermiticity of the system. The eigenenergies are given as,

$$E_\pm = \pm\sqrt{\mathbf{p}^2 - s^2 + 2ip_2 s}. \tag{12}$$

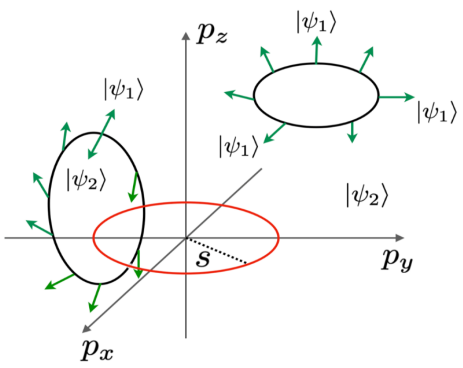

FIG. 2: Mobius Loops in NH Systems [12]

It is clear that the set of EPs here form a disk. Now we again track the wavefunctions along closed loops. See Figure 2 We see that even though one loop does *not* touch any EP point, due to its encirclement we have a mobius loop. This is related to the fact that one needs to make branch cuts in order to make the complex square root function to be analytic in the whole domain.
This elucidates some crucial points of EPs and how they create mobius loops in NH systems that differ from hermitian systems. Particularly, it illustrates how the spectral nature in a NH system is much more intricate and linked to the topology of the bands. Moreover, this hints towards winding of the parameter loops around the EPs.

C. Symmetry Ramifications

The authors of [13] showed that in NH systems, there is a need to redefine the notion of symmetries. Particularly, since for a hermitian hamiltonian we have that $H = H^\dagger$, thus we have $H^* = H^T$. The transpose and the conjugate operations are equivalent. For instance, the Particle Hole Symmetry (PHS) for hermitian sytems can be given as

$$\mathcal{C}H^*\mathcal{C}^{-1} = -H \tag{13}$$

as well as

$$\mathcal{C}H^T\mathcal{C}^{-1} = -H \tag{14}$$

since both are equivalent when $H = H^\dagger$. Similarly for Chiral Symmetry (CS) in hermitian systems we have,

$$\Gamma H\Gamma^{-1} = -H \Leftrightarrow \Gamma H^\dagger\Gamma^{-1} = -H \tag{15}$$

his has a non-trivial implication – many times the topology of the bands and the existence of edge states is intimately linked with symmetries manifested in the hamiltonian. Thus, there is a need to reevaluate symmetry classes when moving to the NH arena. The interested reader may see [13] for a full exposition.

III. GEOMETRIC PHASE IN NH SYSTEMS

We follow the approach in [10]. With the usual ansatz for a parametrized hamiltonian $H \equiv H(\mathbf{R})$, wherein $\mathbf{R} \equiv \mathbf{R}(t)$, we write the evolution of states as,

$$|\psi(t)\rangle = \sum_n c_n(t)\exp\left\{\frac{-\iota}{\hbar}\int_0^t E_n(t')dt'\right\}|\psi_R^n(t)\rangle \tag{16}$$

Substituting into the TDSE, we have,

$$\begin{aligned}\iota\hbar\sum_n \dot{c}_n(t)\exp\left\{\frac{-\iota}{\hbar}\int_0^t E_n(t')dt'\right\}|\psi_R^n(t)\rangle + \\ \iota\hbar\sum_n c_n(t)\exp\left\{\frac{-\iota}{\hbar}\int_0^t E_n(t')dt'\right\}\left|\dot{\psi}_R^n(t)\right\rangle = 0\end{aligned} \tag{17}$$

Dotting both sides with $\langle\psi_L^m|$, we get

$$\begin{aligned}\dot{c}_m(t) = -c_m(t)\langle\psi_L^m \mid \psi_R^m\rangle - \\ \sum_{n\neq m} c_n(t)\langle\psi_L^m \mid \psi_R^n\rangle\exp\left\{\iota\int_0^t \omega_{mn}(t')dt'\right\}\end{aligned} \tag{18}$$

Where, $\omega_{mn}(t) = (E_m(t) - E_n(t))/\hbar$. We assume that we started in the m^{th} state. Clearly, if the energies are complex, these $\exp\{\omega\}$ terms can blow up. Thus we conclude that the Berry Phase is only meaningful if we have the reality of eigenvalues. Based on the work done on $\mathcal{PT}$ Symmetric Hamiltonians with unbroken $\mathcal{PT}$ symmetry we can take this for granted (see introduction and appendix A).
Now, noting that, $\langle\psi_L^m \mid \psi_R^n\rangle \sim \langle\psi_R^m, \psi_R^n\rangle_X$ (as discussed in the previous section) and assuming that the adiabatic theorem holds, we have,

$$\dot{c}_m = -c_m\langle\psi_L^m \mid \dot{\psi}_R^m\rangle \tag{19}$$

This gives us,

$$\begin{aligned}c_m(t) &= \exp\left\{-\int_0^t \langle\psi_L^m(t') \mid \dot{\psi}_R^m(t')\rangle dt'\right\} \\ &= \exp\left\{\iota\left(\int_0^t \iota\langle\psi_L^m(t') \mid \dot{\psi}_R^m(t')\rangle dt'\right)\right\} \\ &= \exp\left\{\iota\left(\int \iota\langle\psi_L^m(\mathbf{R}) \mid \nabla_{\mathbf{R}}\psi_R^m(\mathbf{R})\rangle\cdot d\mathbf{R}\right)\right\}\end{aligned} \tag{20}$$

Thus we have the expression for the berry vector potential, and the berry curvature as,

$$\begin{aligned}\mathbf{A}_m &= \iota\langle\psi_L^m(\mathbf{R}) \mid \nabla_{\mathbf{R}}\psi_R^m(\mathbf{R})\rangle \\ \mathbf{B}_m &= \nabla\times\mathbf{A}_m \\ &= \iota\langle\nabla\psi_L^m \mid \times \mid \nabla\psi_R^m\rangle\end{aligned} \tag{21}$$

Now, one can note that,

$$\begin{aligned}\langle\psi_R^m \mid X \mid \psi_R^m\rangle &= \langle\psi_L^m \mid \psi_R^m\rangle \\ &= \delta_{mn}\end{aligned} \tag{22}$$

Differentiating this equation w.r.t. $\mathbf{R}$, we conclude that the berry phase is only real if

$$\langle \psi_R^m \mid (\nabla_{\mathbf{R}} X) \mid \psi_R^m \rangle = 0 \tag{23}$$

Thus, in addition to demanding reality of eigenvalues, this condition should also be fulfilled for a real geometric phase.
Connecting the notion of the NH berry curvature in this section and EPs in NH systems in the previous sections, the authors of [10, 12] showed that the NH berry curvature has zero divergence as long as the eigenstates are well defined and smooth. Thus *monopoles* of NH systems include branch cuts as well as EPs. We defer a detailed discussion on this for the interested reader to [12].

IV. NH SKIN MODES AND FAILURE OF BBC

A. Numerical Investigations

We conduct thorough numerical investigations to provide insight into the skin effect and the failure of BBC in NH systems by working with a NH SSH chain, wherein non-hermiticity has been imposed through two ways,

1. Non-reciprocity: We change the intracell hopping t_1 to $t_1 \pm \Delta$ in the forward and reverse directions. Similarly, we change t_2 to $t_2 \pm \Delta$.

2. Staggered Imaginary Potential: We add $\pm \iota u$ terms at the A and B sites respectively.

Here, we show the results of the standard SSH chain with $N = 50$ unit cells, and compare it with the results obtained in the non-reciprocative SSH chain with $\Delta = 0.2$. The value of $t_2 = 1$ and t_1 is varied to get the plots. We plot both the absolute energy spectrum of both the open and closed chains in blue and grey respectively.

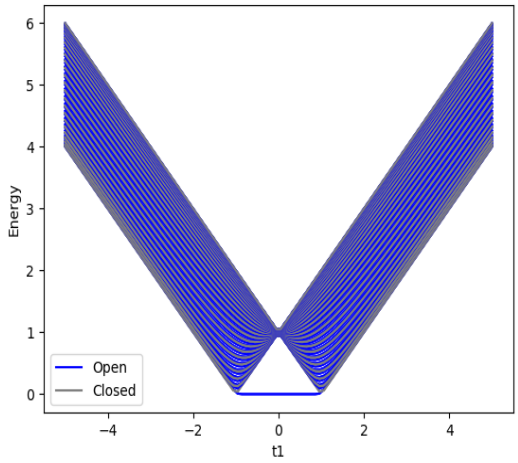

FIG. 3: Standard SSH Energy Plot

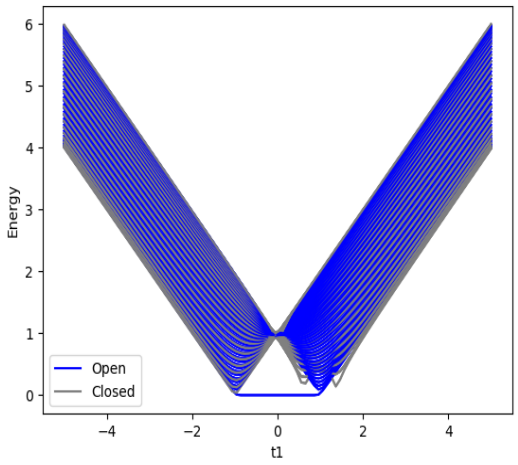

FIG. 4: NH-SSH Energy Plot with $\Delta = 0.2$

In the standard SSH case, we (as expected) see that the band touchings ($E = 0$ points) of the periodic spectrum faithfully signal the existence of edge modes (Figure 3). But, in the $\Delta = 0.2$ case (Figure 4) we see that the periodic spectrum is *not* clearly indicating the existence of open edge modes. This simple example illustrates the breakdown of BBC in the NH case.
Now, we plot the probability densities $|\psi|^2$ of 10 (out of $50 \times 2 = 100$) randomly selected eigenstates in both the case. We see a starking results - 6), while we see normal random states for the standard case (Figure 5). This is a clear example of the NHSE! We defer the other plots (for the other cases) to the appendix.

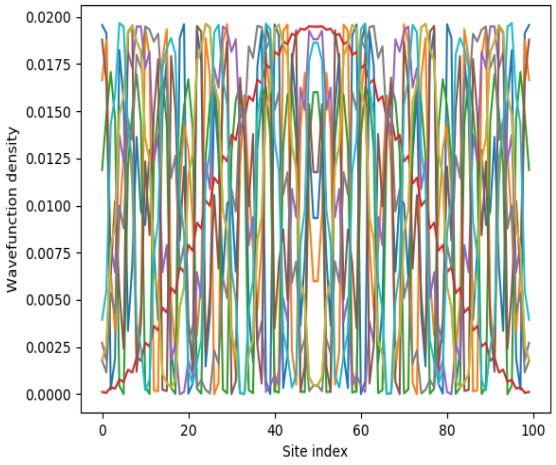

FIG. 5: Standard SSH Density Plot

It is interesting to note that a very similar model has been realized experimentally using topoelectric circuits in [14] wherein they implemented hermitian coupling us-

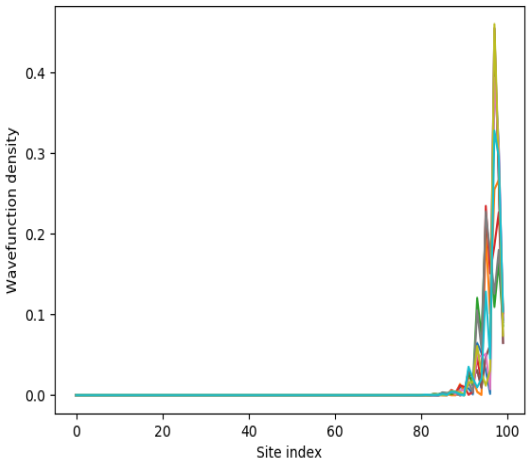

FIG. 6: NH-SSH Density Plot with $\Delta = 0.2$

ing LC oscillators and introduced non-hermiticity using opamps to drive gain into the system.

B. The NH-BBC

Seeing the failure of the conventional BBC in NH systems, there have been efforts and intuition driving towards such a correspondence tailored to NH systems. The work done in [15] [16]] showed the same for *single band models*, with possible extensions to multi band models.

The idea is to define the hamiltonian as a holomorphic function on some open set in $\mathbb{C}$. The physical intuition is that, there can be resistance to deformations only if some quantity akin to the band gap exist in NH systems. This gap can be a *point gap* in a NH system, in the sense that there exists some $E_b \in \mathbb{C}$ such that $E(k) \neq E_b$ for all $k \in BZ$. Usually the choice of this E_b is motivated by the presence of symmetries, but we will let it be general for the analysis here. Consider the tight binding hamiltonian,

$$\begin{aligned} H &= \sum_{i,j} t_{i,j} \left|i\right\rangle \left\langle j\right| \\ H &= \sum_{k \in BZ} H(k) \left|k\right\rangle \left\langle k\right| \end{aligned} \tag{24}$$

Where we usually have,

$$H(k) = \sum_{r} t_r(\exp\{\iota k\})r \tag{25}$$

The key idea now is that we let $\beta := \exp\{\iota k\}$ be a general complex number, as done in [17] [15]. As a concrete case, let us have the case that $t_{i,j} \equiv t_{i-j}$ is non-zero only for $-m \leq i - j \leq n$, we get

$$H(\beta) = t_{-m}\beta^{-}m + \cdots + t_n\beta^n = \frac{P(\beta)}{\beta^m} \tag{26}$$

As one would guess, we would be concerning ourselves with the winding number given as,

$$w(E_b) = \frac{1}{2\pi} \oint_C \frac{d}{dz} \arg[H(z) - E_b] dz \tag{27}$$

But, we know that taking $C = BZ$ does not give us fruitful results in the NH case. Thus, following [17] we now derive the *General Brilloin Zone* (GBZ). There are two steps,

1. Solve the algebraic equation
$$\det(H(\beta) - E) = 0$$
2. Order the solutions, such that $|\beta_i| \leq |\beta_{i+1}|$.

Now we make the following definition,

Definition 1 (GBZ) *For the hamiltonian $H(\beta)$ with solutions to the determinant equation $|\beta_1| \leq |\beta_2| \leq \ldots$ define the GBZ as the following set in the complex plane,*

$$GBZ := \{\beta \mid |\beta_m(H(\beta))| = |\beta_{m+1}(H(\beta))|\} \tag{28}$$

Note that the m in the definition is related to the fact that $H(\beta)$ has a pole of order m at the origin. The profoundess of this seemingly artificial definition is that one can compute the open boundary spectrum of a NH system of large (infinite) size by evaluating on the GBZ instead of the BZ. For the Hermitian case, this again reduces to the unit circle in the complex plane (as $|\exp\{\iota k\}| = 1 \forall k$). Further, we have the following theorem,

Theorem 1 (GBZ Theorem) *The GBZ is that closed contour in the complex plane which encircles the pole of order m at the origin and exactly m zeros of the polynomial $P(z) - Ez^m$ for any $E \in \mathbb{C}$.*

The consequence of this result is that there exists no winding of any complex energy in the mapped contour on the energy plane (by using Cauchy's Residue Principle). The OBC spectrum collapeses into a line, as seen in the figure.

Further, the paper [15] claims that each point $\beta \in$ GBZ represents an eigenstate $|\psi(\beta)\rangle$ such that

$$\langle s \mid \psi(\beta)\rangle = \mathcal{O}(|\beta|^s) \tag{29}$$

where s labels the site index. Thus, unless the GBZ = BZ always, we have that skin modes always exists (at $s = 1$ if $|\beta| < 1$ or at $s = L$ if $|\beta| > 1$). In extreme cases wherein the GBZ lies entirely inside or entirely outside the BZ all the bulk modes are skin modes!

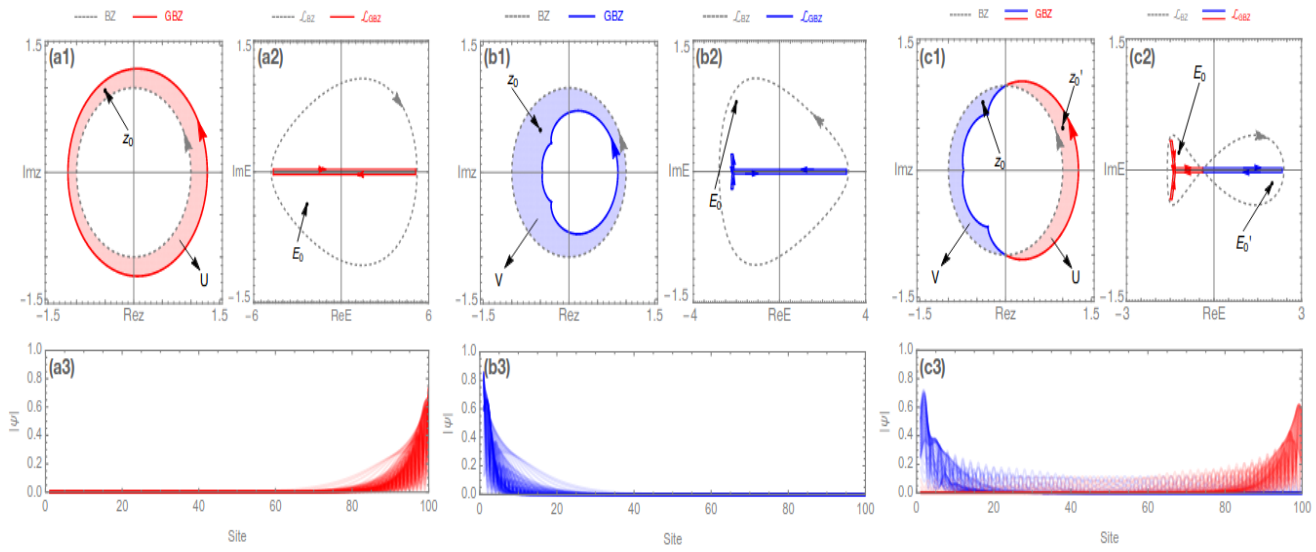

FIG. 7: [15] GBZ, BZ and spectra for different hamiltonians $H(z) = z^{-2}/5+3z^{-1}+2z$, $H(z) = z^{-2}/5+z^{-1}+2z$ and $H(z) = 2z^{-2}/5 + z^{-1} + z$

V. MODELS

A. Exact Boundary Modes in NH Models

The work in [18] derives a polarization operator approach to classifying topological phases in 1-D NH systems. The usual two level hamiltonian is

$$H = \mathbf{d} \cdot \sigma \tag{30}$$

They consider the case of a SSH-like chain, but impose that the last unit cell is broken – ie, it terminates at site A at both ends. Then, defining $d_x \pm \iota d_y = f_\pm + g_\pm \exp\{\pm \iota k a\}$ there exists exact solutions with support only on A sites (in the biorthonormal system as before)

$$\begin{aligned} |\psi_R\rangle &= \mathcal{N}_R \sum_{n=1}^{N} r_R^n c_{A,n}^\dagger |0\rangle \;\; r_R = \frac{-f_+}{g_+} \\ |\psi_K\rangle &= \mathcal{N}_L \sum_{n=1}^{N} r_L^n c_{A,n}^\dagger |0\rangle \;\; r_L = \frac{-f_+^*}{g_+^*} \end{aligned} \tag{31}$$

One finds that

$$\mathcal{N}_L^* \mathcal{N}_R = (r_L^* r_R)^{-1}(r_L^* r_R - 1)/[(r_L^* r_R)^N - 1] \tag{32}$$

If one considers the projector $\Pi_n = |e_{A,n}\rangle \langle e_{A,n}| + |e_{B,n}\rangle \langle e_{B,n}|$ one finds that for the exact solution we get,

$$\langle \Pi_n \rangle = \langle \psi_L \mid \Pi_n \mid \psi_R \rangle = \mathcal{N}_L^* \mathcal{N}_R (r_L^* r_R)^n \tag{33}$$

This indicates exponential localization to either cell $i = 1$ ($|r_L^* r_R| < 1$) or $i = N$ ($|r_L^* r_R| > 1$) unless at the transition point

$$|r_L^* r_R| = 1 \tag{34}$$

Using this criticality condition which correctly predicts the behaviour of boundary localization a quantity called biorthogonal polarization P is coined, such that,

$$P = 1 - \lim_{N\to\infty} (\langle \psi_L \mid \frac{\sum_n n \Pi_n}{N} \mid \psi_R \rangle \tag{35}$$

which exhibits a quantized jump precisely at the points of criticality. Further, this can be extended to models which cannot be exactly solved. The model used in the above figure has

$$d_x(k) = t_1 + t_2 \cos k \;;\; d_y(k) = \iota\gamma/2 + t_2 \sin k \;;\; d_z(k) = 0 \tag{36}$$

B. Chiral and Chiral Broken NH SSH Models

This work done in [19] uses berry formalism developed for NH system in section 2 as well as the same model as our numerical investigations to explain the winding number in NH systems.

$$\begin{aligned} H^{\text{hop}} &= v_1 \sum_{n=1}^{N} |n,B\rangle\langle n,A| + v_2 \sum_{n=1}^{N} |n,A\rangle\langle n,B| \\ &+ w_1 \sum_{n=1}^{N-1} |n+1,A\rangle\langle n,B| + w_2 \sum_{n=1}^{N-1} |n,B\rangle\langle n+1,A| \end{aligned} \tag{37}$$

In addition to the hopping, we will consider an imaginary staggered potential when discussing the $\mathcal{PT}$ symmetric case, given by the term

$$H^{\text{pot}} = iu \sum_{n=1}^{N} (|n,A\rangle\langle n,A| - |n,B\rangle\langle n,B|). \tag{38}$$

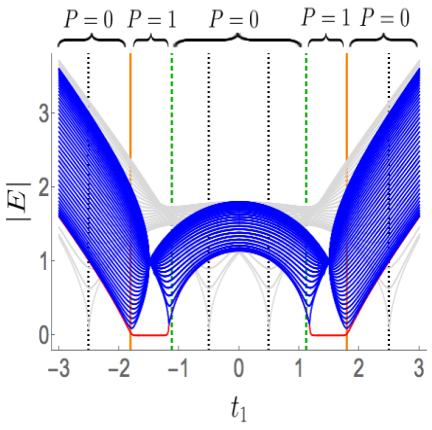

FIG. 8: Absolute spectra of NH SSH model. The gray lines indicate the periodic Bloch bands while the qualitatively different spectra in blue (bulk) and red (edge) correspond to the open system. The orange (dark green dashed) vertical lines indicate where $r_L^* r_R = 1$ ($r_L^* r_R = -11$) and the gray dotted-dashed lines correspond to the EPs of the periodic Bloch Hamiltonian. [18]

The full Hamiltonian reads

$$H = H^{\text{hop}} + H^{\text{pot}} \tag{39}$$

The bloch hamiltonian then is

$$\begin{pmatrix} iu & w_1 e^{-ik} + v_2 \\ w_2 e^{ik} + v_1 & -iu \end{pmatrix} \tag{40}$$

The invariant used here is the berry phase defined in section 2, as,

$$Q_n^c = i \int_{BZ} \left\langle \psi_{L,k}^n \middle| \frac{\partial}{\partial k} \middle| \psi_{R,k}^n \right\rangle dk \tag{41}$$

In the $u = 0$ case, we have that the hamiltonian possesses chiral symmetry, given by $\sigma_z H(k) \sigma_z = -H(k)$, which results in $\pm$ energy pairs. Because of this we have that $\left|\psi_R^{\pm}\right\rangle = \sigma_z \left|\psi_R^{\mp}\right\rangle$. Further, this chiral synmmetry implies a conjugated-pseudo symmetry $H^\dagger = \sigma_x H^* \sigma_x$. Because of this, we have that $\left|\psi_L^{\pm}\right\rangle = \sigma \left|\psi_R^{\pm}\right\rangle$. Combining the two, we parametrize

$$\begin{aligned} \left|\psi_k^{\pm}\right\rangle &= \frac{1}{\sqrt{2 \sin\theta_k \cos\theta_k}} \begin{pmatrix} e^{-i\phi_k} \cos\theta_k \\ \pm \sin\theta_k \end{pmatrix} \\ \left|\lambda_k^{\pm}\right\rangle &= \frac{1}{\sqrt{2 \sin\theta_k \cos\theta_k}} \begin{pmatrix} e^{-i\phi_k} \sin\theta_k \\ \pm \cos\theta_k \end{pmatrix} \end{aligned} \tag{42}$$

Using this, we see that,

$$Q_{\pm}^c \in \{0, \pm 1\} \tag{43}$$

For the staggered potential $u \neq 0$ $\mathcal{PT}$ symmetric case, we use the theory in [20] along with the expression for the new berry phase to arrive at the following phase diagram.

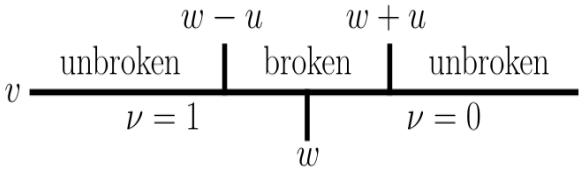

FIG. 9: One-dimensional phase diagram in v for the $\mathcal{PT}$ symmetric case $v_1 = v_2 = v \in \mathbb{R}$, $w_1 = w_2 = w \in \mathbb{R}$. The system moves in and out of the $\mathcal{PT}$ broken phase as a function of v. ν is the topological index which predicts how many pairs of gapless-real-energy, edge modes exist in the system. The bulk spectrum is gapless in the entire $\mathcal{PT}$ -broken phase. [19]

VI. CONCLUSION

To summarise, in this review we briefly discussed how the notion of non-hermiticity brings in interesting arguments and rich topological structure, which is far from norm in the hermitian case. We talked about a fundamentally new phenomenon, the NHSE and the breakdown of the conventional arguments in the BBC. The simple mathematical insights brought on by the analysis of biorthogonal systems, exceptional points and NH mobius loops and monopoles sets one up with tools to think further – to describe 2D and 3D NH systems. We also reviewed some established theoretical and empirical results in NH systems, new notions of polarization operators and NH winding numbers, and the GBZ, which upon careful inspection would set up the ground for further unification of the theory of non-hermitian topological insulators.

ACKNOWLEDGMENTS

We thank Prof. Bhaskaran Muralidharan and Prof. Ashwin Tulapurkar for interesting and insightful lectures throughout the course in Topological Electronics run at IIT Bombay. Additionally, we are grateful to our classmates for helpful discussions.

[1] C. M. Bender, Introduction to PT-Symmetric Quantum Theory, Contemporary Physics **46**, 277 (2005), arXiv:quant-ph/0501052.

[2] L. Lu, J. D. Joannopoulos, and M. Soljačić, enTopological photonics, Nature Photonics **8**, 821 (2014), number: 11 Publisher: Nature Publishing Group.

[3] I. Rotter, enA non-Hermitian Hamilton operator and the physics of open quantum systems, Journal of Physics A: Mathematical and Theoretical **42**, 153001 (2009).

[4] H. Cao and J. Wiersig, Dielectric microcavities: Model systems for wave chaos and non-Hermitian physics, Reviews of Modern Physics **87**, 61 (2015), publisher: American Physical Society.

[5] H. Shen and L. Fu, Quantum Oscillation from In-Gap States and a Non-Hermitian Landau Level Problem, Physical Review Letters **121**, 026403 (2018), publisher: American Physical Society.

[6] [1509.02295] A Short Course on Topological Insulators: Band-structure topology and edge states in one and two dimensions ().

[7] S.-Q. Shen, W.-Y. Shan, and H.-Z. Lu, enTopological insulator and the Dirac equation, SPIN **01**, 33 (2011), arXiv:1009.5502 [cond-mat].

[8] D. C. Brody, enBiorthogonal Quantum Mechanics, Journal of Physics A: Mathematical and Theoretical **47**, 035305 (2014), arXiv:1308.2609 [math-ph, physics:quant-ph].

[9] A. V. Sokolov, A. A. Andrianov, and F. Cannata, enNon-Hermitian quantum mechanics of non-diagonalizable Hamiltonians: puzzles with self-orthogonal states, Journal of Physics A: Mathematical and General **39**, 10207 (2006).

[10] Q. Zhang and B. Wu, Non-Hermitian quantum systems and their geometric phases, Physical Review A **99**, 032121 (2019), publisher: APS.

[11] E. J. Bergholtz, J. C. Budich, and F. K. Kunst, Exceptional topology of non-Hermitian systems, Reviews of Modern Physics **93**, 015005 (2021), publisher: APS.

[12] Q. Zhang and B. Wu, Monopoles in non-Hermitian systems, Journal of Physics A: Mathematical and Theoretical **53**, 065203 (2020), publisher: IOP Publishing.

[13] K. Kawabata, K. Shiozaki, M. Ueda, and M. Sato, Symmetry and topology in non-Hermitian physics, Physical Review X **9**, 041015 (2019), publisher: APS.

[14] Generalized bulk–boundary correspondence in non-Hermitian topolectrical circuits | Nature Physics ().

[15] K. Zhang, Z. Yang, and C. Fang, enCorrespondence between Winding Numbers and Skin Modes in Non-Hermitian Systems, Physical Review Letters **125**, 126402 (2020).

[16] Z. Gong, Y. Ashida, K. Kawabata, K. Takasan, S. Higashikawa, and M. Ueda, Topological phases of non-Hermitian systems, Physical Review X **8**, 031079 (2018), publisher: APS.

[17] K. Yokomizo and S. Murakami, enNon-Bloch Band Theory of Non-Hermitian Systems, Physical Review Letters **123**, 066404 (2019).

[18] F. K. Kunst, E. Edvardsson, J. C. Budich, and E. J. Bergholtz, Biorthogonal bulk-boundary correspondence in non-Hermitian systems, Physical review letters **121**, 026808 (2018), publisher: APS.

[19] S. Lieu, enTopological phases in the non-Hermitian Su-Schrieffer-Heeger model, Physical Review B **97**, 045106 (2018), arXiv:1709.03788 [cond-mat].

[20] Phys. Rev. A 87, 012118 (2013) - Topological invariance and global Berry phase in non-Hermitian systems ().

[21] F. Song, S. Yao, and Z. Wang, Non-Hermitian topological invariants in real space, Physical review letters **123**, 246801 (2019), publisher: APS.

[22] S. Yao and Z. Wang, Edge states and topological invariants of non-Hermitian systems, Physical review letters **121**, 086803 (2018), publisher: APS.

[23] H. Shen, B. Zhen, and L. Fu, Topological band theory for non-Hermitian Hamiltonians, Physical review letters **120**, 146402 (2018), publisher: APS.

[24] N. Okuma, K. Kawabata, K. Shiozaki, and M. Sato, Topological origin of non-Hermitian skin effects, Physical review letters **124**, 086801 (2020), publisher: APS.

[25] D. S. Borgnia, A. J. Kruchkov, and R.-J. Slager, Non-Hermitian boundary modes and topology, Physical review letters **124**, 056802 (2020), publisher: APS.

[26] A. Ghatak and T. Das, New topological invariants in non-Hermitian systems, Journal of Physics: Condensed Matter **31**, 263001 (2019), publisher: IOP Publishing.

[27] X.-D. Cui and Y. Zheng, Geometric phases in non-Hermitian quantum mechanics, Physical Review A **86**, 064104 (2012), publisher: APS.

[28] A. A. Mailybaev, O. N. Kirillov, and A. P. Seyranian, Geometric phase around exceptional points, Physical Review A **72**, 014104 (2005), publisher: APS.

[29] X. Z. Zhang and Z. Song, Geometric phase and phase diagram for a non-Hermitian quantum X Y model, Physical Review A **88**, 042108 (2013), publisher: APS.

[30] G. Dattoli, R. Mignani, and A. Torre, Geometrical phase in the cyclic evolution of non-Hermitian systems, Journal of Physics A: Mathematical and General **23**, 5795 (1990), publisher: IOP Publishing.

[31] Y. Xiong, Why does bulk boundary correspondence fail in some non-hermitian topological models, Journal of Physics Communications **2**, 035043 (2018), publisher: IOP Publishing.

[32] V. M. Alvarez, J. B. Vargas, and L. F. Torres, Non-Hermitian robust edge states in one dimension: Anomalous localization and eigenspace condensation at exceptional points, Physical Review B **97**, 121401 (2018), publisher: APS.

[33] M. Ezawa, Electric circuits for non-Hermitian Chern insulators, Physical Review B **100**, 081401 (2019), publisher: APS.

[34] Y.-X. Xiao and C. T. Chan, Topology in non-Hermitian Chern insulators with skin effect, Physical Review B **105**, 075128 (2022), publisher: APS.

[35] Y. Chen and H. Zhai, Hall conductance of a non-Hermitian Chern insulator, Physical Review B **98**, 245130 (2018), publisher: APS.

[36] S. Yao, F. Song, and Z. Wang, Non-hermitian chern bands, Physical review letters **121**, 136802 (2018), publisher: APS.

[37] C. Yin, H. Jiang, L. Li, R. Lü, and S. Chen, enGeometrical meaning of winding number and its characterization of topological phases in one-dimensional chiral non-Hermitian systems, Physical Review A **97**, 052115

(2018), arXiv:1802.04169 [cond-mat].
[38] W. D. Heiss, Exceptional points of non-Hermitian operators, Journal of Physics A: Mathematical and General **37**, 2455 (2004), publisher: IOP Publishing.
[39] T. Stehmann, W. D. Heiss, and F. G. Scholtz, Observation of exceptional points in electronic circuits, Journal of Physics A: Mathematical and General **37**, 7813 (2004), publisher: IOP Publishing.
[40] K. Ding, G. Ma, M. Xiao, Z. Q. Zhang, and C. T. Chan, Emergence, coalescence, and topological properties of multiple exceptional points and their experimental realization, Physical Review X **6**, 021007 (2016), publisher: APS.
[41] M.-A. Miri and A. Alù, Exceptional points in optics and photonics, Science **363**, eaar7709 (2019), publisher: American Association for the Advancement of Science.
[42] W. D. Heiss, The physics of exceptional points, Journal of Physics A: Mathematical and Theoretical **45**, 444016 (2012), publisher: IOP Publishing.
[43] A. Marie, H. G. Burton, and P.-F. Loos, Perturbation theory in the complex plane: exceptional points and where to find them, Journal of Physics: Condensed Matter **33**, 283001 (2021), publisher: IOP Publishing.
[44] C. Li, X. Z. Zhang, G. Zhang, and Z. Song, enTopological phases in Kitaev chain with imbalanced pairing, Physical Review B **97**, 115436 (2018), arXiv:1707.04718 [cond-mat, physics:quant-ph].
[45] D. Halder, S. Ganguly, and S. Basu, enProperties of the non-Hermitian SSH model : role of PT-symmetry (2022), arXiv:2209.13838 [cond-mat, physics:quant-ph].
[46] V. M. M. Alvarez, J. E. B. Vargas, M. Berdakin, and L. E. F. F. Torres, enTopological states of non-Hermitian systems, The European Physical Journal Special Topics **227**, 1295 (2018), arXiv:1805.08200 [cond-mat, physics:quant-ph].

Appendix A: $\mathcal{PT}$ Symmetry

The Parity Operator $\mathcal{P}$ and the Time Reversal Operator $\mathcal{T}$ are one of the fundamental discrete symmetries in quantum mechanics. The parity operator essentially transforms $\hat{x} \to -\hat{x}$ and $\hat{p} \to -\hat{p}$ and is unitary. The time reversal operator, usually a notorious one to define, transforms $\hat{x} \to \hat{x}$, $\hat{p} \to -\hat{p}$ *and* $\iota \to -\iota$. It is anti-unitary.
Symmetries in quantum mechanics are manifested in the hamiltonians. A hamiltonian is symmetric under the transformation $\mathcal{O}$ if we have that

$$[H, \mathcal{O}] = 0$$

The work in [1] showed that a hamiltonian with 'unbroken' $\mathcal{PT}$ symmetry always has real eigenvalues and implies unitary evolution. Note that the $\mathcal{PT}$ operator is *anti-linear*. That is, $[H, \mathcal{PT}] = 0$ does *not* imply that H and $\mathcal{PT}$ have the same spectrum. Thus, we say that a hamiltonian has unbroken $\mathcal{PT}$ symmetry if it is $\mathcal{PT}$ symmetric and all its eigenfunctions are eigenfunctions of the $\mathcal{PT}$ operator too. If the former but not the latter, we say that the hamiltonian has broken $\mathcal{PT}$ symmetry.

Appendix B: Diagonalization

For a given matrix $H \in \mathbb{C}^{n\times n}$, recall that the *characteristic polynomial* is defined as,

$$det(H - xI) = 0$$

Now, for each eigenvalue λ of H, we define the two quantities

Definition 2 (Algebraic Multiplicity) *The algebraic multiplicity of λ is defined as the greatest natural number n such that $(x-\lambda)^n$ devides the characteristic polynomial. It is denoted a_λ.*

Definition 3 (Geometric Multiplicity) *The geometric multiplicity of λ is defined as the dimension of the nullspace of the matrix $H - \lambda I$. This is denoted g_λ*

We have that the following theorem holds,

Theorem 2 (Theorem) *Given $H \in \mathbb{C}^{n\times n}$, let Λ be the set of its eigenvalues. Then,*

1. *$g_\lambda \leq a_\lambda$ holds $\forall \lambda \in \Lambda$.*
2. *H is diagonalizable over $\mathbb{C}$ if and only if*

$$g_\lambda = a_\lambda$$

holds for all $\lambda \in \Lambda$. Further, we have that,

$$\sum_{\lambda\in\Lambda} a_\lambda = n$$

Appendix C: Numerical Plots

Herein we provide the rest of the plots that were obtained in course of the numerical investigation of the NH-SSH chain.

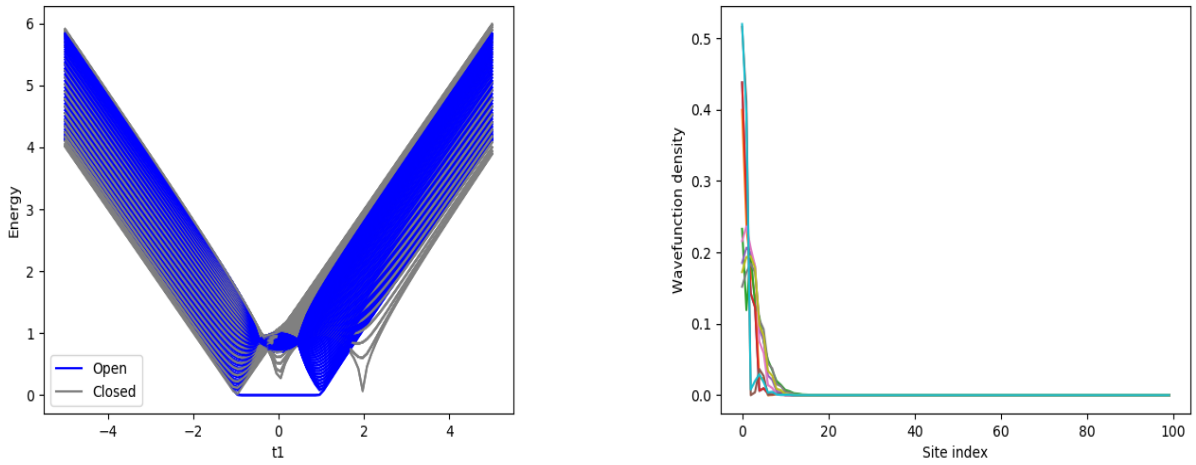

FIG. 10: Energy and density plots for $u = 0, \Delta = 0.5$

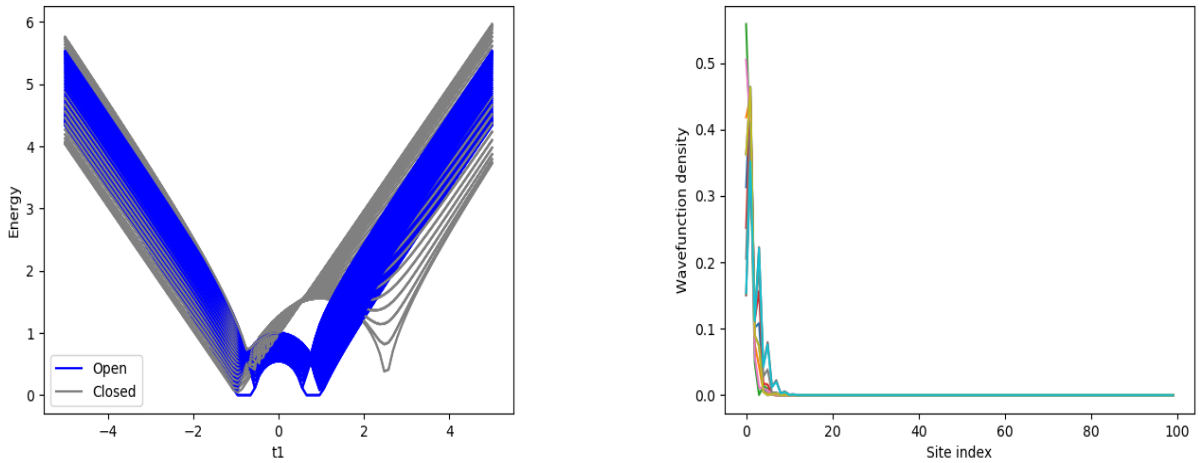

(a) u=0delta=0.8state Plot

FIG. 11: Energy and density plots for $u = 0, \Delta = 0.8$

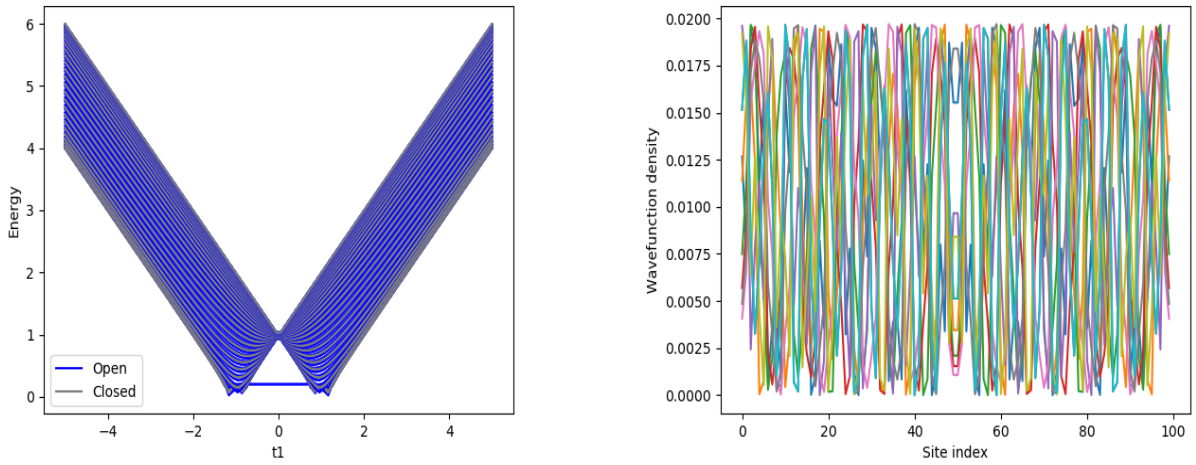

FIG. 12: Energy and density plots for $u = 0.2, \Delta = 0$

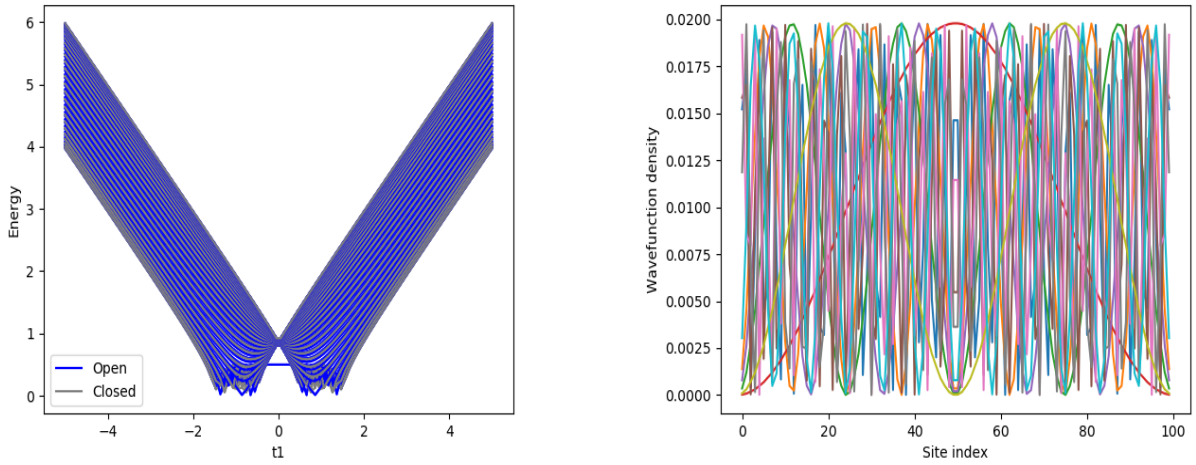

FIG. 13: Energy and density plots for $u = 0.5, \Delta = 0$

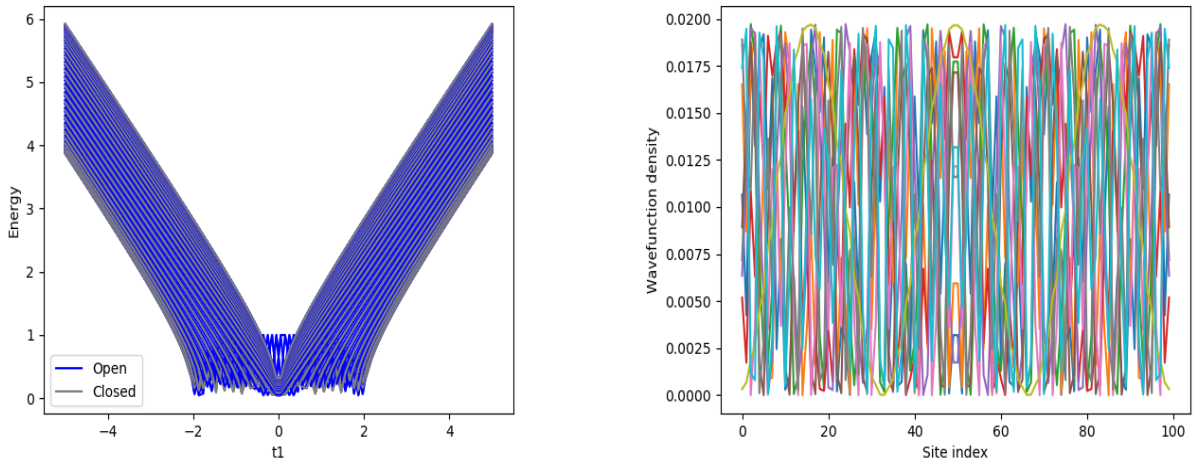

FIG. 14: Energy and density plots for $u = 1, \Delta = 0$

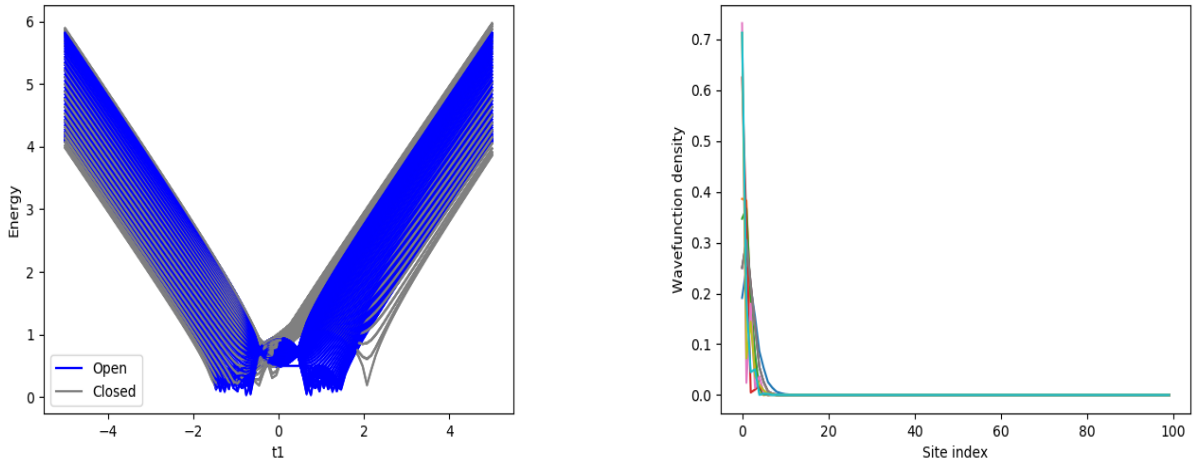

FIG. 15: Energy and density plots for $u = 0.5, \Delta = 0.5$